Journal of Molecular Structure 1002 (2011) 1–9

Contents lists available at ScienceDirect

Journal of Molecular Structure

journal homepage: www.elsevier.com/locate/molstruc

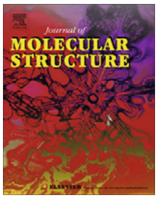

Conformational properties of $F_2S{=}N{-}CF_2{-}N{=}SF_2$ and $F_2S{=}N{-}CF_2{-}N{=}S(O)F_2$: Vibrational spectra and quantum chemical calculations

Andrea Flores Antognini [a], Norma L. Robles [a], Edgardo H. Cutin [a,*], Heinz Oberhammer [b,*]

[a] INQUINOA, Facultad de Bioquímica, Química y Farmacia, Universidad Nacional de Tucumán, Ayacucho 471, (4000) Tucumán, Argentina
[b] Institut für Physikalische und Theoretische Chemie, Universität Tübingen, 72076 Tübingen, Germany

ARTICLE INFO

Article history:
Received 12 January 2011
Received in revised form 14 March 2011
Accepted 15 March 2011
Available online 21 March 2011

Keywords:
Bis(N-difluorosulfurimino)difluoromethane
N-difluorosulfurimino-N-difluorosulfuroxyimino difluoromethane
Conformational properties
Vibrational spectra
Quantum chemical calculations

ABSTRACT

The structural and conformational properties of $F_2S{=}N{-}CF_2{-}N{=}SF_2$ and $F_2S{=}N{-}CF_2{-}N{=}S(O)F_2$ were studied by vibrational spectroscopy (IR(gas) and Raman(liquid)) and by quantum chemical calculations, using B3LYP and MP2 methods with small and large basis sets. Since the SF_2 and $S(O)F_2$ groups can adopt *syn* (s) or *anti* (a) position (*syn*/*anti* of the F—S—F bisector with respect to the adjacent N—C bond) and the orientation around the two N—C bonds can be *trans* (t) or *gauche* (g), a large number of possible conformers is expected. In the case of $F_2S{=}N{-}CF_2{-}N{=}SF_2$ calculations with large basis sets predict the presence of a single conformer with both SF_2 groups in *syn* position and *gauche* orientation around both N—C bonds (s–g–g–s conformer). This is confirmed by the vibrational spectra. For $F_2S{=}N{-}CF_2{-}N{=}SF_2$ analysis of the vibrational spectra in combination with the quantum chemical calculations suggests the predominance of the s–g–t–s conformer, i.e. *syn* position of SF_2 and $S(O)F_2$ groups, *gauche* orientation around one N—C bond and *trans* orientation around the other N—C bond, and the presence of a smaller amounts of the s–t–g–s and s–g–g–s conformers.

1. Introduction

The study of the structural properties of molecules containing NS bonds is of great interest, since different conformations may occur due to different electronic and steric effects. Such compounds are not only interesting because of their bonding properties [1], but they also have been used as intermediates in the synthesis of many useful compounds for pharmacological applications [2–4]. Recently, a sulfilimine bond (—N=S<) has been identified in a biomolecule, arising from the reaction between the side chains of two amino acids in collagen IV [5]. The presence of lone pairs at nitrogen and sulfur atoms plays an important role in the biochemical reduction which gives a sulfenamide compound, as well as in oxidation reactions resulting in sulfoximine derivatives (—N=S(O)<).

The study of the conformational and vibrational properties of molecules possessing the $-N{=}SF_2$ and $-N{=}S(O)F_2$ moieties is a matter of great importance in the chemistry of fluorinated sulfur–nitrogen compounds. From the conformational point of view, the properties of substances containing the $-N{=}SF_2$ moiety are unique. For all sulfurdifluoride imides of the type $R{-}N{=}SF_2$ with R = Cl [6], CF_3 [7], FSO_2 [8], FC(O) [9], CN [10] and $CF_3C(O)$ [11] only a single conformer with *syn* orientation of the R—N bond with respect to the F—S—F bisector (see Chart 1) was observed experimentally in the fluid phases. These experimental results are confirmed by quantum chemical calculations which predict the energies of *anti* conformers to be higher by about 2–10 kcal/mol. The much higher stability of the sterically unfavorable *syn* form has been rationalized through the concept of anomeric effects. Orbital interactions between the electron lone pairs of sulfur and nitrogen with the σ^* orbitals of the N—R and S—F bonds, respectively, are much stronger in the *syn* structure than in the *anti* form and overcompensate steric effects [9].

On the other hand, in the respective S(VI) homologs sulfuroxidedifluoride imides of the type $R{-}N{=}S(O)F_2$ with R = Cl [12], FC(O) [13,14], FSO_2 [15], N≡C [16,17], SF_5 [18] as well as $O{=}C(N{=}S(O)F_2)_2$ [19] both conformers, *syn* and *anticlinal* (see Chart 2) can occur in the fluid phases. Although the most stable configuration of all these compounds still possesses *syn* orientation of the N—R bond relative to the F—S—F bisector (see Chart 2), small contributions (10–25%) of an additional conformer were observed experimentally by gas electron diffraction and/or vibrational spectroscopy in the case of $FC(O)N{=}S(O)F_2$ and $SF_5N{=}S(O)F_2$. This second stable structure in the fluid phases possesses sterically adequate *anticlinal* orientation of the F—S—F bisector relative to the N—R bond, which corresponds to *synclinal* orientation of the S=O bond with respect to the N—R bond. Quantum chemical calculations predict for these compounds a smaller energy difference between *syn* and *anti* conformers of about 1–2 kcal/mol. The lower

---

* Corresponding authors.
E-mail addresses: cutin@fbqf.unt.edu.ar (E.H. Cutin), heinzoberhammer@uni-tuebingen.de (H. Oberhammer).

0022-2860/$ - see front matter © 2011 Published by Elsevier B.V.
doi:10.1016/j.molstruc.2011.03.033

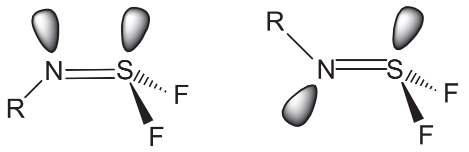

syn *anti*

Chart 1.

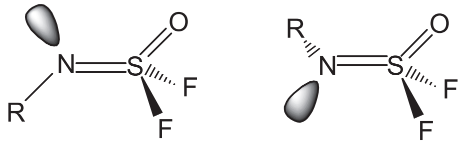

syn *anticlinal*

Chart 2.

relative stability of the *syn* form can be rationalized by reduced anomeric effects due to the absence of the lone electron pair at the sulfur atom.

A detailed computational analysis of $N\equiv SF_2-N=SF_2$ and $N\equiv SF_2-N=S(O)F_2$, two compounds which possess a single, double and triple NS bond, was reported recently [20]. For both molecules structures with *cis* or *trans* orientation of the $N\equiv S-N=S$ moiety and with *syn* or *anti* configuration of the SF_2 or $S(O)F_2$ groups are feasible. Chart 3 shows the four possible conformers for $N\equiv SF_2-N=S(O)F_2$. According to vibrational spectroscopy and quantum chemical calculations, only the *cis–syn* conformer is present in both compounds with *cis* structure of the $N\equiv S-N=S$ chain and *syn* orientation of the SF_2 or $S(O)F_2$ groups, respectively.

In this context, we now report a structural, conformational and vibrational study for $F_2S=N-CF_2-N=SF_2$ and $F_2S=N-CF_2-N=S(O)F_2$, based on vibrational spectra [FTIR (gas) and Raman (liquid)] and on quantum chemical calculations at different levels of theory. These two molecules contain either two $-N=SF_2$ moieties or one $-N=SF_2$ and one $-N=S(O)F_2$ group, bridged by CF_2. Due to different possible orientations around the two N=S and N—C bonds a complex potential energy surface is expected. Although numerous conformations are feasible, it is clear from the vibrational spectra, that a rather limited number of forms are actually present in the fluid phases. In order to assess the molecular structure of the title compounds, a theoretical study of the potential energy surface has been carried out by systematic variation of torsional angles around both N—C and S=N bonds, using the B3LYP and MP2 methods with small and large basis sets.

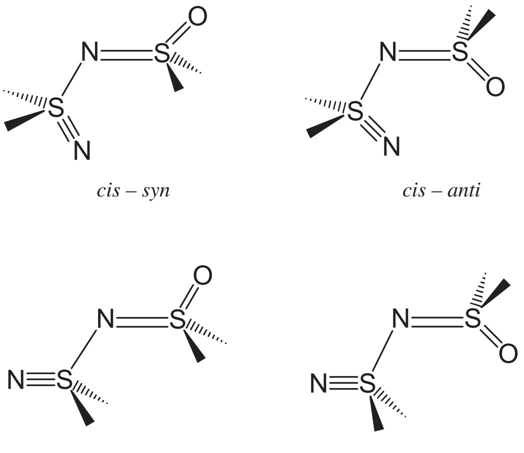

cis – syn *cis – anti*

trans – syn *trans –anti*

Chart 3.

2. Experimental details

$F_2S=N-CF_2-N=SF_2$ and $F_2S=N-CF_2-N=S(O)F_2$ were synthesized by the reaction of $N\equiv C-N=SF_2$ and $N\equiv C-N=S(O)F_2$ with SF_4, respectively [21,22]. The products were purified at reduced pressure by repeated trap-to-trap distillations at low temperatures. The gas FTIR spectra were registered between 4000 and 400 cm^{-1} (resolution 2 cm^{-1}) with a Perkin Elmer Paragon 500 FT IR spectrometer, using a 10 cm path-length cell equipped with KBr windows. The liquid Raman spectrum of $F_2S=N-CF_2-N=S(O)F_2$ was recorded between 2000 and 50 cm^{-1} using a Jobin Ivon U1000 Spectrometer equipped with both Argon and Krypton ion lasers (Spectra Physics Model 165), and radiation of 514.5 nm (Ar^+) was used for excitation with an argon ion laser (Spectra Physics model 165). The liquid samples were handled in glass capillaries at room temperature. The Raman spectrum of $F_2S=N-CF_2-N=SF_2$ could not be recorded due to decomposition of the liquid sample at room temperature.

3. Quantum chemical calculations

Structural and conformational properties as well as vibrational spectra for $F_2S=N-CF_2-N=SF_2$ and $F_2S=N-CF_2-N=S(O)F_2$ were studied with different quantum chemical methods using the GAUSSIAN 03 program package [23]. Rather complex conformational properties are expected for these compounds since two orientations around each S=N bond (*syn* (s) or *anti* (a) orientation of the SF_2 and $S(O)F_2$ groups), and at least two orientations around each N—C bond (*trans* (t) and *gauche* (g)) are feasible, resulting in a possible number of $2^4 = 16$ conformers.

3.1. $F_2S=N-CF_2-N=SF_2$

In the first step a search of stable conformations around the two C—N bonds with both SF_2 groups in *syn* position was performed with the B3LYP/6-31G(d) method. The position of the SF_2 groups are described by the dihedral angles θ_1(CN=S1X1) and θ_2(CN=S2X2), with X1 and X2 being dummies at the SF_2 bisectors (see Fig. 1 for atom numbering). Dihedral angles of 0° correspond to exact *syn* position of the SF_2 groups. The 3-dimensional potential surface for the two torsional angles Φ_1(NC—NS1) and Φ_2(NC—NS2) were calculated in steps of 20° in the range of 0–180° (Fig. 2). In this potential surface relative energies for Φ_1 and Φ_2 larger than 60° vary smoothly between 0 and 1 kcal/mol, whereas energies

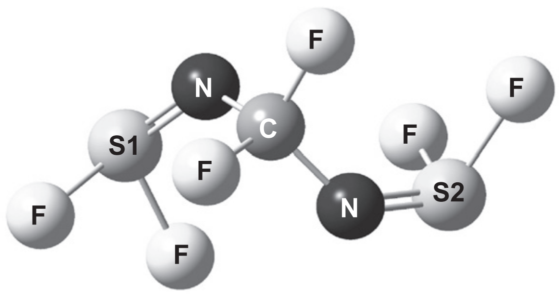

Fig. 1. *Syn–gauche–gauche–syn* structure of $F_2S=N-CF_2-N=SF_2$with atom numbering.

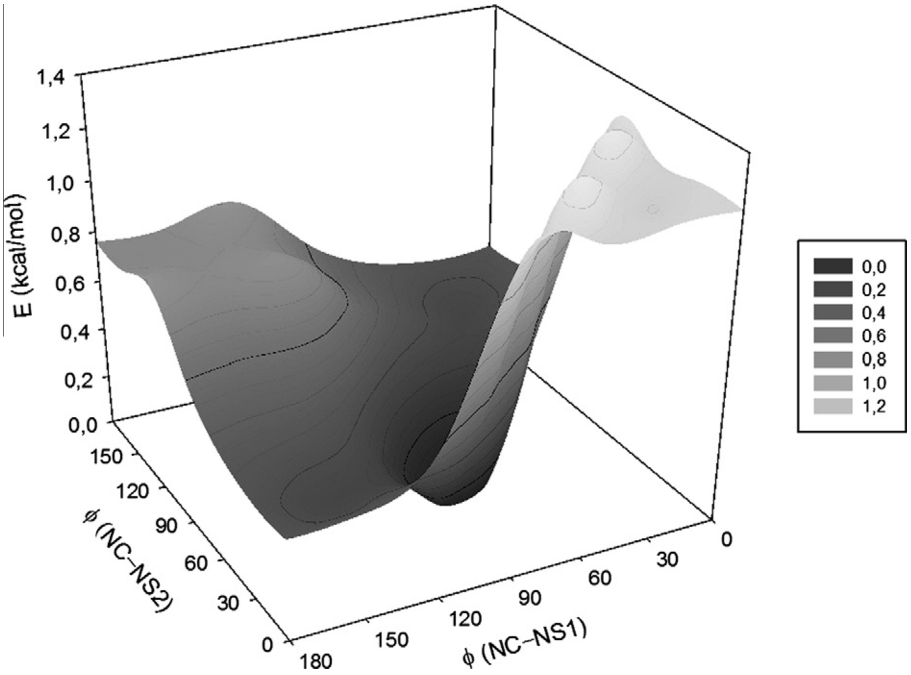

Fig. 2. 3-Dimensional energy surface of $F_2S{=}N{-}CF_2{-}N{=}SF_2$ for the two rotational angles NC—NS1 and NC—NS2 derived with the (B3LYP/6-31G(d) method.

increase steeply for smaller torsional angles. To obtain a better resolution in the low-energy region, all energies larger that 1.2 kcal/mol were set to 1.2 kcal/mol (light gray section in Fig. 2). It should be pointed out that relative energies and some structural parameters derived with the DFT method depend slightly on the gridsize for numerical calculation of integrals. All present calculations were performed with the option "ultrafine gridsize". The potential surface possesses a pronounced minimum for *gauche* orientation around both C—N bonds ($\Phi_1 = \Phi_2 \approx 67°$) and a very shallow minimum for *trans* orientation around both C—N bonds ($\Phi_1 = \Phi_2 \approx 180°$), about 0.7 kcal/mol higher in energy. According to this computational method no minimum exists for a *trans–gauche* conformer. To obtain information about the potential barrier between the *trans–trans* and *gauche–gauche* conformer a one-dimensional potential function for $\Phi_1 = \Phi_2$ along the diagonal of Fig. 2 was calculated in steps of 20° with B3LYP and MP2 method with small (6-31G(d)) and large (cc-pVTZ) basis sets (Fig. 3). All methods predict a distinct minimum for the *gauche–gauche* structure, the shape of the potential function near the *trans–trans* conformer, however, depends on the computational method. B3LYP and MP2 calculations with small basis sets predict a minimum in the *trans–trans* region with barriers to *gauche–gauche* of about 0.19 and 0.33 kcal/mol, respectively. The potential curve obtained with the B3LYP/cc-pVTZ method is extremely flat in the *trans–trans* region with a barrier of only 0.015 kcal/mol to the *gauche–gauche* conformer. This barrier is lower than the zero-point energy of the torsional vibration (12 cm^{-1}) and therefore the *trans–trans* conformer is not populated. According to the MP2/cc-pVTZ method no stable *trans–trans* conformer exists. Both calculations with large basis sets suggest that only a *gauche–gauche* conformer is expected to be observed.

In the next step all feasible structures with both SF_2 groups in *syn* position, i.e. *gauche–gauche* (s–g–g–s), *trans–trans* (s–t–t–s) and *trans–gauche* (s–t–g–s) were fully optimized with B3LYP and MP2 methods using small and large basis sets (see Chart 4 for molecular models). The dihedral angles around the C—N and N=S bonds, relative energies and free energies and predicted mol

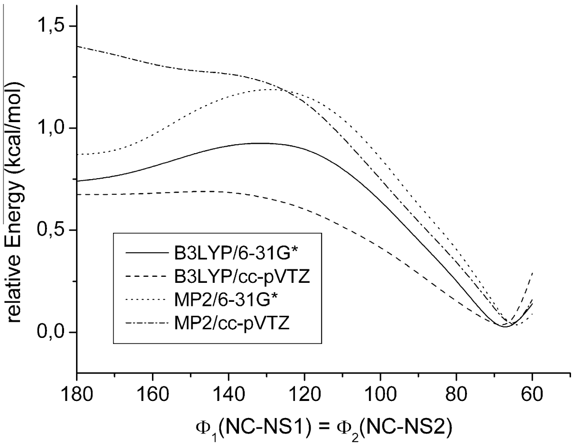

Fig. 3. Potential curve for $\Phi_1 = \Phi_2$ (diagonal of Fig. 1) derived with different computational methods.

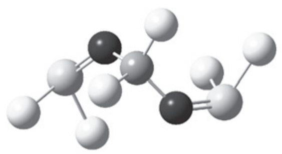

syn – gauche – gauche – syn

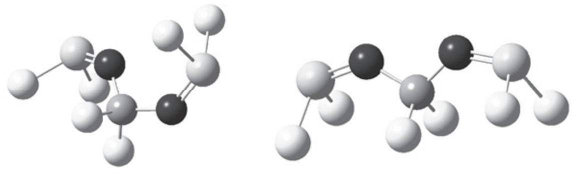

syn – trans – gauche – syn   *syn – trans – trans – syn*

Chart 4.

Table 1
Torsional angles around C—N and N═S bonds, relative energies, free energies and mol fractions for stable conformers of $F_2S{=}N{-}CF_2{-}N{=}SF_2$ with both SF_2 groups in *syn* position, derived with different computational methods.

Conformer	NC—NS1	NC—NS2	CN═SX1[a]	CN═SX2[a]	ΔE [b]	ΔG^{0}[b]	mol%
s–g–g–s[c]							
B3LYP/sb[d]	66.6	66.6	−0.4	−0.4	0.00	0.00	33
B3LYP/lb[d]	67.8	67.8	−0.6	−0.6	0.00	0.00	49
MP2/sb	63.2	63.2	−0.9	−0.9	0.00	0.00	11
MP2/lb	64.2	64.2	−0.4	−0.4	0.00	0.00	100
s–t–t–s[c]							
B3LYP/sb	180.0	180.0	0.0	0.0	0.74	−0.43	67
B3LYP/lb	180.0	180.0	0.0	0.0	0.66	−0.03	51
MP2/sb	177.4	177.4	−1.0	−1.0	0.87	−1.07	66
MP2/lb	–	–	Not stable	–	–	–	0
s–t–g–s[c]							
B3LYP/sb			Not stable				0
B3LYP/lb			Not stable				0
MP2/sb	165.8	76.4	−4.2	−2.4	0.75	−0.43	23
MP2/lb			Not stable				0

[a] X1, X2 are dummy atoms on the F—S—F bisectors of the SF_2 groups.
[b] kcal/mol.
[c] s is *syn* position of SF_2 groups, g/t is *gauche/trans* orientation around the C—N bonds.
[d] sb = 6-31G(d), lb = cc-pVTZ.

fractions of stable conformers are collected in Table 1. It has to be pointed out that free energies are calculated in the Gaussian program with the assumption of deep harmonic wells for each conformer. This leads to unrealistic values for ΔG^0 and mol fractions in the case of very shallow minima occurring in our case. With this assumption the B3LYP/lb calculation predict the presence of 51% s–t–t–s conformer, although this conformer is not populated due to the small barrier.

All computational methods predict a stable s–g–g–s conformer which possesses the lowest energy. The calculated geometric parameters for this stable structure are listed in Table 2. Both calculations with small basis sets predict also a stable s–t–t–s structure, about 0.7–0.9 kcal/mol higher in total energies, but lower in free energies by 0.4–1.1 kcal/mol. These large differences between energies and free energies are due to much lower frequencies for the torsional vibrations in the s–t–t–s conformer compared to those in the s–g–g–s structure. The MP2/6-31G(d) method predicts torsional vibrations of 22 and 33 cm^{-1} for the s–g–g–s structure and unreasonably low frequencies of 4 and 8 cm^{-1} for the s–t–t–s form, resulting in much higher entropies for the s–t–t–s conformer. Thus, ΔG^0 values have to be taken with great care. Only the MP2/6-31G(d) approximation predicts the presence of a stable s–t–g–s conformer with *trans–gauche* orientation of the SN–C–NS chain. Again, the barrier to the lower energy s–g–g–s conformer is very low, leading to a much lower actual population as predicted by the G^0 value.

An additional search for stable conformers with one or both SF_2 groups in *anti* position (θ_1 or θ_1 and $\theta_2 \approx 180°$) was performed using the B3LYP/6-31G(d) method. These calculations resulted in four additional stable structures (a–g–g–s, a–c–t–s, a–g–g–a and a–c–t–a), two of which possesses *cis* (c) orientation of the S═N—C—N chain. Since relative free energies of these conformers are much higher (4–9 kcal/mol) than those for structures with both SF_2 groups in *syn* position, they will not be observable in the experiment and no further calculations with other methods were performed.

3.2. $F_2S{=}N{-}CF_2{-}N{=}S(O)F_2$

Similar calculations (B3LYP with 6-31G(d) and 6-31+G(df) basis sets and MP2 with 6-31+G(df) basis set) were preformed for $F_2S{=}N{-}CF_2{-}N{=}S(O)F_2$. In the first step, the conformational properties around the two N—C bonds were studied with SF_2 and $S(O)F_2$ groups in *syn* orientation. The 3-dimensional energy surface for the two rotational angles Φ_1 (N2C—N1S1) and Φ_2 (N1C—N2S2) in the ranges 0–180° was calculated in steps of 30° with the B3LYP/6-31G(d) method (for atom labeling see Fig. 4). This surface (Fig. 5) possesses a low-energy region for both rotational angles larger than 45° with energies between 0 and 1 kcal/mol, whereas it rises

Table 2
Calculated geometric parameters for the *syn–gauche–gauche–syn* conformer of $F_2S{=}N{-}CF_2{-}N{=}SF_2$.[a].

	B3LYP/cc-pVTZ	MP2/cc-pVTZ
Bond lengths		
C—N	1.429	1.429
N═S	1.495	1.497
S—F	1.635	1.618
C—F	1.354	1.344
Angles		
S═N—C	131.6	129.2
N—C—N	114.4	114.0
N═S—F	110.2	110.3
N—C—F	109.0	108.9
S═N—C—N	67.8	64.2

[a] Bond lengths in Å, angles in degrees. For atom labeling see Fig. 1. For some parameters average values are given.

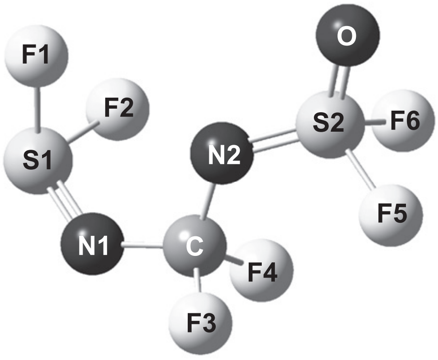

Fig. 4. *Syn–gauche–trans–syn* structure of $F_2S{=}N{-}CF_2{-}N{=}S(O)F_2$with atom numbering.

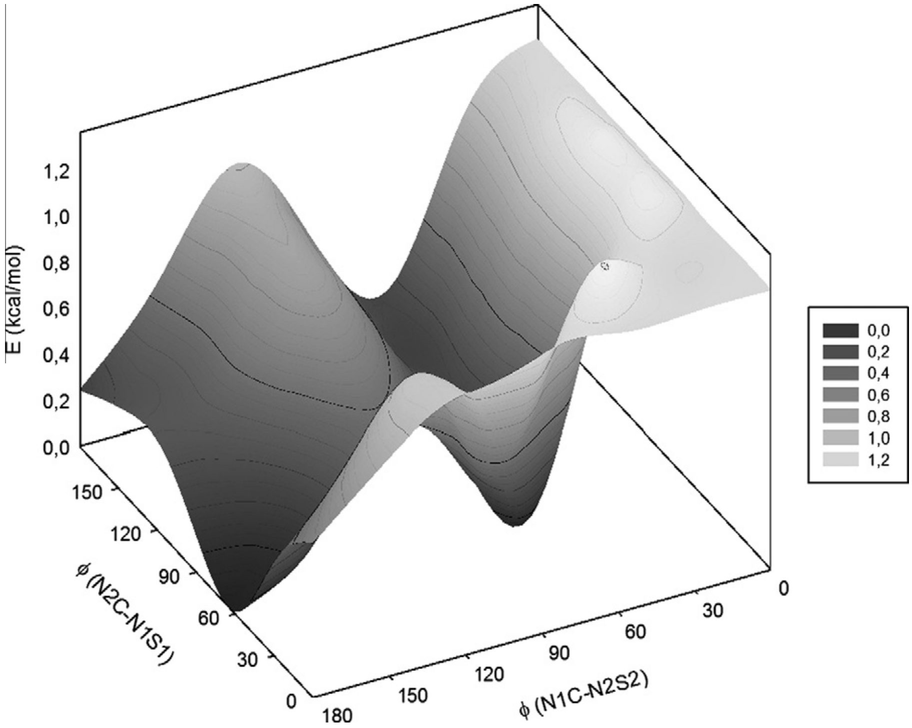

Fig. 5. 3-Dimensional energy surface of $F_2S{=}N{-}CF_2{-}N{=}S(O)F_2$ for the two rotational angles N1C—N2S2 and N2C—N1S1 , derived with the B3LYP/6-31G(d) method.

very steeply for smaller rotational angles with an energy >10 kcal/mol at $\Phi_1 = \Phi_2 = 0°$. As in the case of $F_2S{=}N{-}CF_2{-}N{=}SF_2$, all energies higher than 1.2 kcal/mol were set equal (light gray region of the surface). The potential energy surface possesses four minima for g–t, t–g, g–g and t–t orientation around the two N—C bonds. In the g–g conformation the two sulfur atoms S1 and S2 point into opposite directions of the N—C—N plane. No additional minima occur in the region from 180° to 360° for these rotational angles.

In the second step these four conformations, s–g–g–s, s–t–t–s, s–g–t–s and s–t–g–s (Chart 5), were fully optimized using three computational methods The four torsional angles describing the conformation, the relative energies ΔE and free energies ΔG^0 and mol fractions are summarized in Table 3. Again ΔE and ΔG^0 values differ appreciably for some conformers due to differences in low vibrational frequencies which contribute strongly to the entropies.

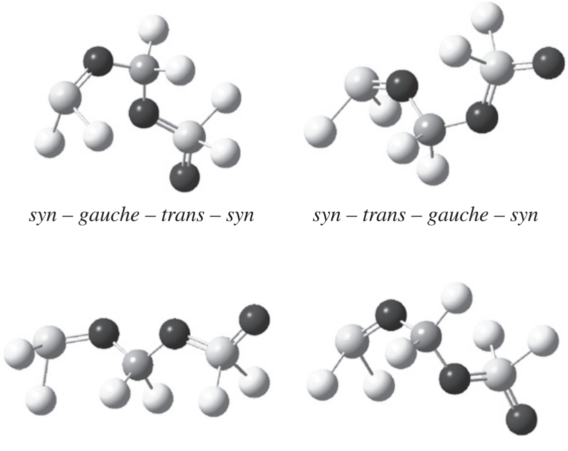

syn – gauche – trans – syn *syn – trans – gauche – syn*

syn – trans – trans – syn *syn – gauche – gauche – syn*

Chart 5.

All methods predict the s–g–t–s conformer with *gauche* orientation around the N1—C and *trans* orientation around the N2—C bond to be the lowest in energy and free energy. The calculated geometric parameters of this conformer are listed in Table 4. The s–t–t–s conformer does not correspond to a stable structure according to the B3LYP/6-31+G(df) method. Furthermore, the 3-dimensional energy surface predicted by the B3LYP/6-31G(d) method (Fig. 5) demonstrates that the potential barrier between the s–t–t–s and s–g–t–s conformers is very low. This results in a much lower actual population of the s–t–t–s conformer at room temperature than that derived from the G^0 value. Thus, calculations indicate that s–g–t–s and s–t–g–s conformers are the main conformers with a possible small contribution of the s–g–g–s form.

Additional calculations for all feasible conformers with SF_2 or/and $S(O)F_2$ groups in *anti* orientation were performed with three computational methods. The B3LYP method with small and large basis sets predicts six additional stable conformers, the MP2 method only five. The free energies of these conformers are 1–6 kcal/mol higher and these conformers are not considered in a further analysis.

4. Vibrational assignment

4.1. $F_2S{=}N{-}CF_2{-}N{=}SF_2$

The FTIR spectrum (gas) of $F_2S{=}N{-}CF_2{-}N{=}SF_2$ is presented in Fig. 6. Observed and calculated wavenumbers, together with a tentative assignment for the 3N – 6 = 27 fundamental modes are listed in Table 5. The vibrational spectrum was assigned for the *syn–gauche–gauche–syn* form (Fig. 1) by comparison with the spectra of related molecules containing the NSF_2 and CF_2 moieties, and on the basis of calculated vibrational frequencies and intensities.

Taking into account the existence of two N=S bonds and the symmetry of this conformer, the two intense bands located at 1390 and 1358 cm^{-1} in the IR spectrum, were assigned to the N=S symmetric and antisymmetric stretching modes, respectively.

Table 3

Dihedral angles, relative energies, free energies and mol fractions of stable conformers of $F_2S{=}N{-}CF_2{-}N{=}S(O)F_2$ predicted by the B3LYP method with small (6-31G(d)) and large (6-31+G(df)) basis sets and by MP2 approximation with large basis sets.

Conformer	C—N1=S1—X1[a]	S1=N1—C—N2	S2=N2—C—N1	C—N2=S2—X2[a]	ΔE [b]	ΔG^{0}[b]	mol%
s–g–t–s[c]							
B3LYP/sb[d]	−1.4	68.5	171.7	−3.5	0.00	0.00	32
B3LYP/lb[d]	−5.3	35.0	170.8	−4.3	0.00	0.00	54
MP2/lb	−7.2	41.6	193.9	8.6	0.00	0.00	38
s–t–g–s[c]							
B3LYP/sb	−3.7	165.4	68.0	−1.4	0.28	0.10	27
B3LYP/lb	−4.4	151.8	45.3	−8.2	0.30	0.32	32
MP2/lb	−4.8	144.5	40.0	−12.1	1.60	0.09	32
s–t–t–s[c]							
B3LYP/sb	1.2	183.3	177.7	−2.9	0.30	0.01	32
B3LYP/lb	–	–	Not stable	–	–	–	0
MP2/lb	5.7	207.9	192.3	7.6	0.62	0.49	16
s–g–g–s[c]							
B3LYP/sb	−0.7	67.6	66.7	−0.7	0.02	0.76	9
B3LYP/lb	1.6	85.1	66.5	−0.3	0.46	0.82	14
MP2/lb	−5.9	48.8	77.6	−0.6	0.06	0.57	14

[a] X1, X2 are dummy atoms on the F—S—F bisectors of the SF_2 and $S(O)F_2$ group, respectively.

[b] in kcal/mol.

[c] First letter describes the orientation of the bisector of the SF_2 group (*syn* or *anti*) relative to N1—C bond. Second letter describes the S1=N1—C—N2 dihedral angle (*trans*, *gauche* or *cis*). Third letter describes the dihedral angle S2=N2—C—N1 (*trans* or *gauche*). Fourth letter describes the orientation of the F—S—F bisector of the $S(O)F_2$ group relative to the N2—C bond.

[d] sb = 6-31G(d), lb = 6-31+G(df).

Table 4

Calculated geometric parameters for the *syn–gauche–trans–syn* conformer of $F_2S{=}N{-}CF_2{-}N{=}S(O)F_2$.[a].

	B3LYP/6-31+G(df)	MP2/6-31+G(df)
Bond lengths		
C—N1	1.422	1.422
C—N2	1.428	1.423
N1=S1	1.502	1.501
N2=S2	1.502	1.498
S2=O	1.431	1.427
[b]S1—F (1 and 2)	1.644	1.634
[b]C—F (3 and 4)	1.365	1.360
[b]S2—F (5 and 6)	1.591	1.580
Angles		
S1=N1—C	133.0	128.9
N1—C—N2	112.3	111.8
S2=N2—C	126.6	123.8
N=S=O	119.0	119.3
[b]N1=S1—F (1 and 2)	110.6	110.6
[b]N1—C—F (3 and 4)	108.2	108.3
[b]N2—C—F (3 and 4)	111.0	111.1
[b]N2=S2—F (5 and 6)	112.2	111.8
[b]O=S—F (5 and 6)	108.4	108.6
S1=N1—C—N2	35.0	41.6
N1—C—N2=S2	170.8	−166.1
C—N=S=O	176.4	−172.3

[a] Bond lengths in Å, angles in degrees. For atom labeling see Fig. 4.

[b] For parameters that are not unique, average values are given.

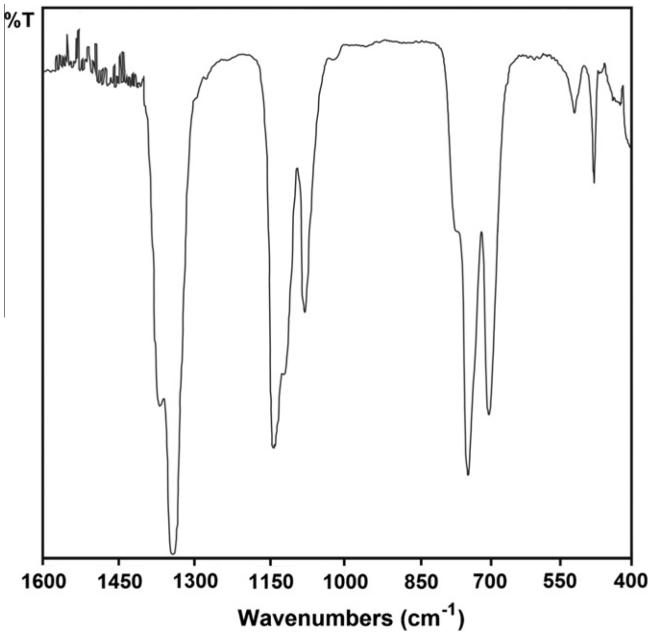

Fig. 6. Gas infrared spectrum of $F_2S{=}N{-}CF_2{-}N{=}SF_2$.

Data reported previously for iminosulfurous compounds of the type $RN{=}SF_2$ [7,9,11] support this assignment.

Vibrational data about the CF_2 stretching is still scarce. As a consequence the assignment of these vibrational modes have been done mainly on the basis of theoretical predictions and by comparison with the experimental spectra of $NS(O)F_2{-}CF_2{-}NS(O)F_2$ [24]. The strong band located at 1152 cm^{-1} in the IR spectra is assigned to the asymmetric stretching of the CF_2 group, while the feature observed at 1128 cm^{-1} is assigned to the symmetric stretching mode of this group. These wavenumbers compare fairly well with the same vibrations found in $NS(O)F_2{-}CF_2{-}NS(O)F_2$ (1154 and 1112 cm^{-1}).

The bands located at 1086 and 705 cm^{-1} were assigned to the antisymmetric and to the symmetric stretching modes of the NCN moiety. This assignment is supported by values found for the same vibrations in $O{=}C(NS(O)F_2)_2$ (1082 and 703 cm^{-1}). The antisymmetric NCN vibration, for which a narrow band occurs in the gas phase spectrum, demonstrates the presence of a single conformer, since a shift of about 30 cm^{-1} to lower wavenumbers is predicted for this vibration in the s–t–t–s conformer and no feature is observed in this region.

According to the observed IR features in other related molecules which posses the NSF_2 group, the symmetric and antisymmetric SF_2 stretching modes appeared in the 800–700 cm^{-1} range. As it was observed previously, the symmetric stretching mode of the

Table 5
Assignments of fundamental modes and experimental and calculated wavenumbers (cm^{-1}) for the *syn–gauche–gauche–syn* conformer of $F_2S{=}N{-}CF_2{-}N{=}SF_2$.

Mode	Approximate description[a]	Experimental[b]	Calculated	
		IR (gas)	B3LYP/cc-pVTZ	MP2/cc-pVTZ
ν_1	N=S sym. stretch.	1390 s	1383 (36)	1413 (46)
ν_2	N=S asym. stretch.	1359 vs	1351 (100)	1395 (100)
ν_3	CF_2 asym. stretch.	1152 s	1138 (35)	1200 (37)
ν_4	CF_2 sym. stretch.	1128 s	1129 (43)	1178 (41)
ν_5	NCN asym. stretch.	1086 m	1059 (30)	1093 (34)
ν_6	$N{=}SF_2$ sym. stretch. i.ph.	776 sh	757 (4)	784 (5)
ν_7	$N{=}SF_2$ sym. stretch. o.o.ph.	750 s	727 (49)	750 (55)
ν_8	NCN sym. stretch.	705 s	713 (1)	728 (<1)
ν_9	$N{=}SF_2$ asym. stretch.	–	678 (5)	707 (26)
ν_{10}	CN=S asym. def.	–	678 (24)	696 (7)
ν_{11}	$N{=}SF_2$ asym. stretch.	–	658 (9)	682 (6)
ν_{12}	NCN def.	–	644 (<1)	666 (<1)
ν_{13}	CN=S sym. def.	524 m	539 (3)	547 (3)
ν_{14}	CF_2 rock.	–	515 (7)	525 (8)
ν_{15}	CF_2 def.	–	473 (1)	484 (1)
ν_{16}	CF_2 wag.	–	433 (1)	452 (1)
ν_{17}	SF_2 def. i.ph.	–	389 (<1)	410 (<1)
ν_{18}	SF_2 def. o.o.ph.	–	358 (1)	375 (1)
ν_{19}	N=SF sym. def. o.o.ph.	–	341 (1)	347 (1)
ν_{20}	CF_2 twist.	–	292 (<1)	297 (1)
ν_{21}	N=SF asym. def. i.ph.	–	238 (<1)	244 (<1)
ν_{22}	N=SF asym. def. o.o.ph	–	131 (<1)	143 (<1)
ν_{23}	$N{=}SF_2$ sym. def. i.ph.	–	130 (<1)	134 (<1)
ν_{24}	Torsion C—N asym.	–	121 (1)	126 (1)
ν_{25}	Torsion N=S asym.	–	76 (<1)	83 (<1)
ν_{26}	Torsion N=S sym.	–	21 (<1)	36 (<1)
ν_{27}	Torsion C—N sym.	–	14 (<1)	12 (<1)

[a] stretch. = stretching; def. = deformation; sym. = symmetric; asym. = antisymmetric; i.ph. = in phase; o.o.ph. = out of phase; rock. = rocking; wagg. = wagging; twist. = twisting. For atom numbering, see Fig. 1.

[b] vs = very strong; s = strong; m = medium; sh = shoulder.

SF_2 group is localized at higher wavenumbers than the corresponding antisymmetric one. Due to the fact that the molecule in study contains two terminal SF_2 groups, the bands centered at 750 and 776 cm^{-1} in the IR spectra were assigned to the in phase symmetric stretching mode of the SF_2 groups and to the out of phase stretching mode of these groups. This assignment is in complete agreement with those previously reported for $FC(O)N{=}SF_2$, $CF_3N{=}SF_2$ and $CF_3CF_2N{=}SF_2$ [9,7,25]. The antisymmetric stretching modes were not observed in the experimental spectrum. The deformations involving the $N{=}SF_2$ and the CF_2 groups are strongly coupled and their assignment is tentative.

4.2. $F_2S{=}N{-}CF_2{-}N{=}S(O)F_2$

The FTIR spectrum (gas) and the Raman spectrum (liquid) obtained for this compound are presented in Figs. 7 and 8, observed and calculated wavenumbers, together with a tentative assignment for the 3N – 6 = 30 fundamental modes are listed in Table 6. Although calculations predict similar contributions of s–g–t–s and s–t–g–s conformers, only the calculated wavenumbers of the s–t–g–s conformer are given in Table 6, since almost all calculated shifts of wavenumbers between the four conformers with both, SF_2

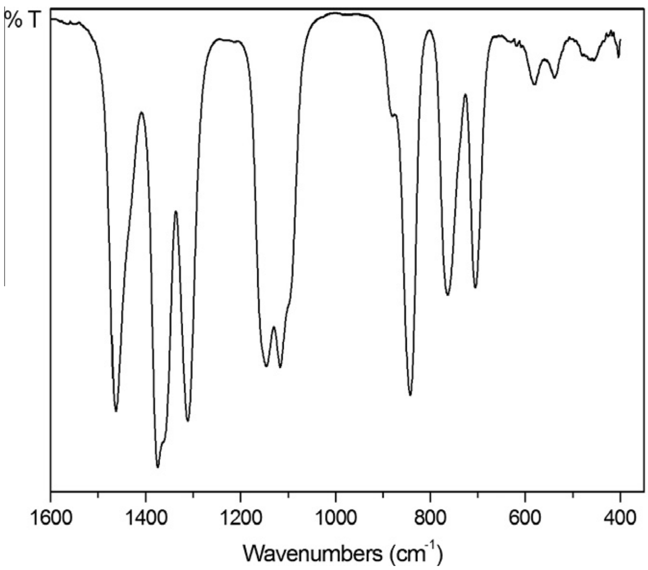

Fig. 7. Gas infrared spectrum of $F_2S{=}N{-}CF_2{-}N{=}S(O)F_2$ (P = 3 torr).

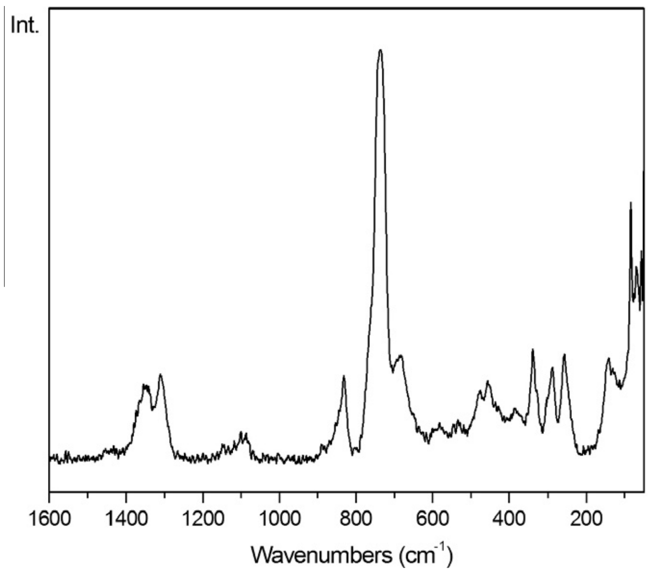

Fig. 8. Liquid Raman spectrum of $F_2S{=}N{-}CF_2{-}N{=}S(O)F_2$.

Table 6
Assignments of fundamental modes and experimental and calculated wavenumbers (cm^{-1}) for the *syn–gauche–trans–syn* conformer of $F_2S{=}N{-}CF_2{-}N{=}S(O)F_2$.

	Approx. description[a]	Experimental[b]		Calculated	
		IR (gas)	Raman (liquid)	B3LYP/6-31+G(df)	MP2/6-31+G(df)
ν_1	N=S=O asym. stretch.	1463 s	1433 vw	1408 (50)[c] [46][d]	1463 (58) [22]
ν_2	N1=S1 stretch.	1375 vs	1355 m	1370 (100) [25]	1420 (100) [37]
ν_3	N=S=O sym. stretch.	1312 s	1311 m	1269 (46) [100]	1327 (40) [73]
ν_4	C—F3 stretch.	1146 s	1150 vw	1131 (42) [4]	1186 (38) [6]
ν_5	C—F4 stretch.	1116 s	1100 vw	1090 (42) [7]	1143 (45) [5]
ν_6	C—N2 stretch.	1097 sh	1087 vw	1078 (23) [7]	1123 (19) [9]
ν_7	N=S(O)F_2 sym. stretch.	882 sh	870 vw	808 (23) [4]	835 (23) [2]
ν_8	N=S(O)F_2 asym. stretch.	842 s	832 m	801 (26) [11]	833 (28) [9]
ν_9	N=SF_2 sym. stretch.	763 m	–	726 (21) [48]	751 (5) [100]
ν_{10}	C—N1 stretch.	–	737 vs	718 (12) [97]	741 (24) [24]
ν_{11}	N=SF_2 asym. stretch.	705 m	687 m	669 (21) [19]	690 (21) [18]
ν_{12}	N1—C—N2 o.o.p def.	631 vw	637 w	638 (1) [13]	668 (<1) [12]
ν_{13}	N1—C—N2 i.p. def.	618 vw	–	608 (5) [10]	622 (3) [2]
ν_{14}	N1—C—N2 sym. def.	581 w	582 vw	572 (1) [12]	598 (5) [17]
ν_{15}	N=S(O)F_2 sym. def.	538 w	534 vw	522 (3) [6]	527 (2) [4]
ν_{16}	N1—C—N2 asym. def.	478 vw	476 w	494 (1) [3]	500 (<1) [3]
ν_{17}	CF_2 sym. def.	460 vw	458 w	454 (6) [15]	471 (7) [11]
ν_{18}	N=S=O o.o.p. def.	454 vw	–	424 (2) [4]	442 (1) [4]
ν_{19}	N=S(O)F_2 sym. def.	434 vw	–	413 (1) [5]	430 (1) [7]
ν_{20}	N=SF_2 sym. def.	404 vw	387 vw	371 (1) [4]	388 (1) [4]
ν_{21}	N=S(O)F_2 sym. def.	–	338vw	315 (<1) [4]	326 (<1) [3]
ν_{22}	N=SF_2 asym. def.	–	328 m	310 (1) [6]	315 (1) [6]
ν_{23}	N=S(O)F_2 asym. def.	–	289 m	264 (<1) [7]	274 (<1) [5]
ν_{24}	N=SF_2 asym. def.	–	258 m	244 (1) [6]	247 (1) [6]
ν_{25}	C—N2=S2 def.	–	142 m	136 (<1) [2]	146 (<1) [1]
ν_{26}	N=SF_2 asym. def.	–	131 m	108 (<1) [<1]	116 (<1) [1]
ν_{27}	N=S(O)F_2 asym. def.	–	85 m	79 (<1) [2]	98 (<1) [<1]
ν_{28}	S1=N1—C def.	–	70 m	74 (<1) [2]	66 (<1) [2]
ν_{29}	Torsion	–	–	18 (<1) [<1]	17 (<1) [<1]
ν_{30}	Torsion	–	–	15 (<1) [<1]	14 (<1) [<1]

[a] stretch. = stretching; def. = deformation; sym. = symmetric; asym. = antisymmetric; i.p. = in plane; o.o.p. = out of plane. For atom numbering, see Fig. 4.
[b] vs = very strong; s = strong; m = medium; w = weak; vw = very weak; sh = shoulder.
[c] Infrared intensities.
[d] Raman activities.

and $S(O)F_2$ groups in *syn* orientation are small (less than 10 cm^{-1} for strong bands) and therefore not observable in the experimental spectra.

Three intense bands are observed in the gas IR spectra in the region between 1500 and 1300 cm^{-1}. As observed for molecules containing the $N{=}S(O)F_2$ group the N=S and the S=O stretching modes are strongly coupled. The antisymmetric stretching mode could be assigned to the signal centered at 1463 cm^{-1} in the infrared spectra (1433 cm^{-1}, Raman) while the feature located at 1312 cm^{-1} in the IR spectra (1311 cm^{-1}, Raman) stands for the N=S=O symmetric stretching mode. The corresponding observed bands for $FC(O)N{=}S(O)F_2$ [13,14], $N{\equiv}CN{=}S(O)F_2$ [16,17] and $O{=}C(N{=}S(O)F_2)_2$ [19] are in complete agreement with this assignment. The most intense IR band at 1375 cm^{-1} (1355 cm^{-1}, Raman) was assigned to the N1=S1 stretching mode. Data reported for $CF_3N{=}SF_2$, $CF_3CF_2N{=}SF_2$ and $CF_3C(O)N{=}SF_2$ confirm this proposal [7,25,11]. According to theoretical predictions, this fundamental mode is predicted at lower frequencies ($\Delta\nu$ = 18 or 21 cm^{-1}, MP2 and B3LYP respectively) for the s–t–g–s conformer. Thus, the signal at 1362 cm^{-1} ($\Delta\nu$ = 13 cm^{-1}), together with the slightly asymmetric shape of the N=S=O antisymmetric stretching (predicted $\Delta\nu$ = 6 or 2 cm^{-1}, MP2 and B3LYP respectively) could indicate the presence of the s–t–g–s conformer. However, no further evidence for this structure, such as splitting of the N=S=O symmetric vibration for which a shift of 17 or 21 cm^{-1} (MP2 and B3LYP, respectively) is predicted, was found in the present study.

The stretching modes of the CF_2 group are strongly affected by its chemical environment. Therefore, the C—F3 stretching mode was assigned to the band located at 1146 cm^{-1} in the IR spectra while the strong band observed at 1116 cm^{-1} could be assigned to the C—F4 stretching fundamental mode. These values agree with those observed for $N{=}SF_2{-}CF_2{-}N{=}SF_2$, where the signals of the C—F stretching modes were found at 1152 and 1128 cm^{-1}.

The N2—C stretching mode can be observed at 1097 in the gas IR and at 1087 cm^{-1} in the liquid Raman spectra. These wavenumbers compare fairly well with the same vibration found in $O{=}C(N{=}S(O)F_2)_2$ (1082 cm^{-1}). The band located at 737 cm^{-1} in the Raman spectrum could be assigned to the N1—C stretching mode, a position which can be compared well with the same mode in $CF_3N{=}SF_2$ [7] and $CF_3CF_2N{=}SF_2$ [25].

As it was mentioned in the vibrational analysis of $F_2S{=}N{-}CF_2{-}N{=}SF_2$, the symmetric stretching modes of the SF_2 group were localized at higher wavenumbers than the corresponding antisymmetric ones. In $F_2S{=}N{-}CF_2{-}N{=}S(O)F_2$, the symmetric stretching mode was assigned to the feature centered at 763 cm^{-1} in the IR spectra while the antisymmetric fundamental was observed in the IR spectra at 705 cm^{-1} (687 cm^{-1}, Raman). Data reported for $FC(O)N{=}SF_2$, $CF_3N{=}SF_2$ and $CF_3CF_2N{=}SF_2$ confirm the proposed assignment [8,7,25]. The SF_2 symmetric stretching mode belonging to the $N{=}S(O)F_2$ moiety, was assigned to the shoulder observed at 882 cm^{-1} in the IR spectra and to the weak band located at 870 cm^{-1} in the Raman spectrum; the antisymmetric stretching was assigned to the band centered at 842 cm^{-1} in the IR spectra (832 cm^{-1}, Raman). Experimental values reported in the literature for $FSO_2N{=}S(O)F_2$ support this proposal [15].

The deformation modes involving the $N{=}SF_2$, $S(O)F_2$ and N1CN2 groups were assigned by comparison with related molecules and on the basis of the predicted wavenumbers by DFT and *ab initio* calculations. Strong couplings between some deformations modes involving the CF_2, the $N{=}SF_2$ and the $S(O)F_2$ groups are derived from the calculated vibrational spectra, and they are tentatively defined as pure deformations of a single group.

5. Conclusion

For $F_2S{=}N{-}CF_2{-}N{=}SF_2$ B3LYP and MP2 calculations with large basis sets predict the presence of a single conformer (*syn–gauche–gauche–syn*) with *syn* configuration of both SF_2 groups and gauche orientation around the two N—C bonds (C_2 symmetry). On the other hand, calculations with small basis sets predict the presence of two additional conformers (s–t–g–s and s–t–t–s). The IR gas spectrum confirms the presence of a single conformer, in agreement with the calculations with large basis sets.

The conformational properties of $F_2S{=}N{-}CF_2{-}N{=}S(O)F_2$ are more complicated. According to B3LYP and MP2 calculations with small and large basis sets three or four low energy conformers with SF_2 and $S(O)F_2$ groups in *syn* position and *gauche* or *trans* orientation around the two N—C bonds exists. All calculations predict s–g–t–s conformer to be lowest in energy, with the s–t–g–s structure being only slightly higher in free energy. The IR gas and Raman liquid spectra are not conclusive whether one or two main conformers are present and the presence of a third conformer with s–g–g–s structure cannot be excluded.

Acknowledgments

Financial support by the Volkswagen Stiftung (I/78 724) and DAAD (Deutscher Akademischer Austauschdienst, Germany) is gratefully acknowledged. The Argentinean authors acknowledge CONICET (Consejo Nacional de Investigaciones Científicas y Técnicas) and UNT (Universidad Nacional de Tucumán). We thank also Prof. R. Mews, University of Bremen, for providing facilities for experimental work.

References

[1] F. Pichierri, Chem. Phys. Lett. 487 (2010) 315.
[2] C. Isambora, D. O'Hagan, J. Fluor. Chem. 127 (2006) 303.
[3] K.L. Kirk, J. Fluor. Chem. 127 (2006) 1013.
[4] J.-P. Bégué, D. Bonnet-Delpon, J. Fluor. Chem. 127 (2006) 902.
[5] R. Vanacore, A.-J.L. Ham, M. Voehler, C.R. Sanders, T.P. Conrads, T.D. Veenstra, K.B. Sharpless, P.E. Dawson, B.G. Hudson, Science 325 (2009) 1230.
[6] J. Haase, H. Oberhammer, W. Zeil, O. Glemser, R. Mews, Z. Naturforsch. 25a (1970) 153.
[7] N.L. Robles, E.H. Cutin, C.O. Della Védova, J. Mol. Struct. 784 (2006) 265.
[8] R.M.S. Alvarez, E.H. Cutin, C.O. Della Védova, Spectrochim. Acta A 58 (2002) 149.
[9] R.M.S. Álvarez, E.H. Cutin, R.M. Romano, C.O. Della Védova, Spectrochim. Acta A 52 (1996) 667.
[10] R.S.M. Alvarez, E.H. Cutin, C.O. Della Védova, R. Mews, R. Haist, H. Oberhammer, Inorg. Chem. 40 (2001) 5188.
[11] M.I. Mora Valdez, E.H. Cutin, C.O. Della Védova, R. Mews, H. Oberhammer, J. Mol. Struct. 607 (2002) 207.
[12] H. Oberhammer, O. Glemser, H. Klüber, Z. Naturforsch. 29a (1974) 901.
[13] N.L. Robles, E.H. Cutin, H. Oberhammer, J. Mol. Struct. 789 (2006) 152.
[14] R. Boese, E.H. Cutin, R. Mews, N.L. Robles, C.O. Della Védova, Inorg. Chem. 44 (2005) 9660.
[15] R.M.S. Alvarez, M.I. Mora Valdez, E.H. Cutin, C.O. Della Védova, J. Mol. Struct. 657 (2003) 291.
[16] R.M.S. Alvarez, E.H. Cutin, H.-G. Mack, O. Sala, C.O. Della Védova, J. Mol. Struct. 328 (1994) 221.
[17] E.H. Cutin, C.O. Della Védova, H.-G. Mack, H. Oberhammer, J. Mol. Struct. 354 (1995) 165.
[18] R.M.S. Álvarez, E.H. Cutin, R. Mews, H. Oberhammer, J. Phys. Chem. A 111 (2007) 2243.
[19] F. Trautner, E.H. Cutin, C.O. Della Védova, H. Oberhammer, J. Mol. Struct. 510 (1999) 53.
[20] A.F. Antognini, N.L. Robles, E.H. Cutin, H. Oberhammer, J. Mol. Struct. 976 (2010) 3.
[21] O. Glemser, U. Biermann, Inorg. Nucl. Chem. Lett. 3 (1967) 223.
[22] O. Glemser, S.P.V. Halasz, Inorg. Nucl. Chem. Lett. 4 (1968) 191.
[23] M.J. Frisch, G.W. Trucks, H.B. Schlegel, G.E. Scuseria, M.A. Robb, J.R. Cheeseman, J.A. Montgomery Jr., T. Vreven, K.N. Kudin, J.C. Burant, J.M. Millam, S.S. Iyengar, J. Tomasi, V. Barone, B. Mennucci, M. Cossi, G. Scalmani, N. Rega, G.A. Petersson, H. Nakatsuji, M. Hada, M. Ehara, K. Toyota, R. Fukuda, J. Hasegawa, M. Ishida, T. Nakajima, Y. Honda, O. Kitao, H. Nakai, M. Klene, X. Li, J.E. Knox, H.P. Hratchian, J.B. Cross, V. Bakken, C. Adamo, J. Jaramillo, R. Gomperts, R.E. Stratmann, O. Yazyev, A.J. Austin, R. Cammi, C. Pomelli, J.W. Ochterski, P.Y. Ayala, K. Morokuma, G.A. Voth, P. Salvador, J.J. Dannenberg, V.G. Zakrzewski, S. Dapprich, A.D. Daniels, M.C. Strain, O. Farkas, D.K. Malick, A.D. Rabuck, K. Raghavachari, J.B. Foresman, J.V. Ortiz, Q. Cui, A.G. Baboul, S. Clifford, J. Cioslowski, B.B. Stefanov, G. Liu, A. Liashenko, P. Piskorz, I. Komaromi, R.L. Martin, D.J. Fox, T. Keith, M.A. Al-Laham, C.Y. Peng, A. Nanayakkara, M. Challacombe, P.M.W. Gill, B. Johnson, W. Chen, M.W. Wong, C. Gonzalez, J.A. Pople, Gaussian, Inc., Wallingford, CT, Revision E.01, 2007.
[24] N.L. Robles, A.F. Antognini, E.H. Cutin, Preliminary results.
[25] N.L. Robles, E.H. Cutin, R. Mews, C.O. Della Védova, J. Mol. Struct. 978 (2010) 131.